

Energy Modelling and Calibration of a Controlled Environment Agriculture Space in a Cold Climate Using Building Performance Simulation Tools

Gilbert Laroche Martin – Hydro-Québec, Canada – larochellemartin.gilbert@hydroquebec.com

Danielle Monfet – École de technologie supérieure, Canada – danielle.monfet@etsmtl.ca

Abstract

This paper presents the energy modelling and calibration of a small-scale experimental greenhouse using building performance simulation tools in a cold climate. The greenhouse is modelled in EnergyPlus using the OpenStudio interface. Evidence-based calibration is then performed using the available construction information. Subsequently, an automated off-line calibration of influent energy model parameters yielded a NMBE of 1.90 % and a CV-RMSE of 5.75 % over monthly energy data. The modelling and calibration conducted in this paper also helped identify knowledge gaps in controlled environment agriculture (CEA) energy modelling using building performance simulation (BPS) tools.

1. Introduction

The Quebec greenhouse sector, covering 313 hectares (3.13 km²), accounts for approximately 1 TWh of annual thermal energy consumption, with around 300 GWh sourced from electricity. With Quebec's government plan to expand greenhouse production, there is a prompt focus on increasing the use of electric energy in the sector. However, as industries strive to decarbonise their production, the demand for low-carbon electricity escalates, resulting in unprecedented pressure on the grid.

Electricity in Quebec, Canada, is primarily produced from very low-carbon renewable sources, mainly hydroelectric dams, owned by Hydro-Québec, a public utility. The greenhouse sector benefits from a reduced rate (6.164 ¢CND·kWh⁻¹) for the electricity used for crop lighting and production space heating. This rate becomes interruptible for about 100 hours per year during cold weather

events, with a higher peak rate applied during those specific periods (58.168 ¢CND·kWh⁻¹). As such, tools are needed to estimate the impacts and propose mitigation strategies for efficient electrification of the greenhouse sector.

Building Performance Simulation (BPS) tools have recently gained popularity for predicting peak energy demand and energy consumption of controlled environment agriculture (CEA) production spaces, including greenhouses and high-density controlled environment agriculture (CEA-HD) production spaces such as vertical farms (e.g., Graamans et al., 2018). The heat balance at the crop canopy level, necessary for proper hygrothermal load prediction in these production spaces, has also been recently implemented into BPS tools. The literature provides limited information regarding the prediction performance of CEA space models developed using BPS tools. Also, the methodology used to calibrate these models has been sparsely addressed in the existing literature (Beaulac et al., 2023).

In this paper, a building energy model of a small-scale experimental greenhouse is developed using design information and in-situ experimental data using the BPS software EnergyPlus. Measurements of the indoor environment conditions and operating data of the energy systems of the CEA production space are used to calibrate the developed BPS model. The data was gathered for an empty greenhouse, i.e., without crops, as the initial step to reduce the number of variables to be calibrated. Finally, the calibrated BPS CEA model prediction is assessed and analysed. This study provides insights into BPS CEA modelling and calibration using case

study data gathered in a northern climate.

2. Description Of The Small-Scale Experimental Greenhouse

The small-scale experimental greenhouse is 6.1 m long by 3.7 m wide and 4.3 m high. The aluminium structure sits on a 0.8 m high by 0.2 m thick concrete wall, as illustrated in Fig. 1 (a). The south-facing windows are double-paned 16 mm glass windows ($RSI=0.33 \text{ m}^2\cdot\text{K}\cdot\text{W}^{-1}$, $\tau=0.9$, $\rho=0.08$), and the north-facing façade consists of 16 mm polycarbonate panels ($RSI=3.2 \text{ m}^2\cdot\text{K}\cdot\text{W}^{-1}$, $\tau=0.62$, $\rho=0.08$). Two operable vents are located on the glass roof. A $1510 \text{ L}\cdot\text{s}^{-1}$ exhaust fan with gravity louvres is located in the gable end opposite the doors, and two operated louvres are beside the entrance door. The electric heating system has a 9 kW boiler that supplies two hydronic circuits, each with 77.7 m of 15.9 mm (5/8") tubing. In addition to the hydronic floor, a 5 kW, $165 \text{ L}\cdot\text{s}^{-1}$ fan coil unit (FCU) is installed in the greenhouse. The lighting system consists of ten LED luminaires (Sollum SF05A – 340 W, $780 \mu\text{mol}\cdot\text{s}^{-1}$). For the 2022 year, the total energy consumption was 32 149 kWh with a 15-minute peak electrical demand of 14.8 kW. The heating degree-days for the greenhouse location in ASHRAE climate Zone 6A are 4837 (Base $18 \text{ }^\circ\text{C}$).

3. Approach And Method

The proposed modelling and calibration methodology includes three successive steps: (1) energy

model development, (2) evidence-based calibration and (3) additional model parameter estimation. The methodology is applied to a small-scale experimental greenhouse as a case study to test the proposed approach.

3.1 Energy Model Development

The greenhouse geometry was modelled using the OpenStudio plugin for Sketchup. The different energy model attributes were then specified in the OpenStudio (Guglielmetti et al., 2011) interface to EnergyPlus (Crawley et al., 2001). The hydronic floor system was modelled as a hot water loop with a «LowTemperatureRadiant:ConstantFlow» object and the FCU as a «UnitHeater». The photoperiod was set from 04:00 to 20:00, and the lighting system availability was adjusted according to an availability schedule throughout the year. The availability schedule was implemented to take into account periods when systems were disconnected due to ongoing commissioning related work in the greenhouse. An availability schedule was also implemented for the FCU for the same purpose. Fig. 1 (b) illustrates the building energy model geometry compared to the experimental greenhouse.

The infiltration was modelled according to Eq.1 where I is the total zone air changes per hour (ACH), I_D is the design ACH, T_z is the thermal zone air temperature ($^\circ\text{C}$), T_∞ is the outside air temperature ($^\circ\text{C}$) and U_∞ is the wind speed ($\text{m}\cdot\text{s}^{-1}$).

$$I = I_D \cdot (A + B \cdot |T_z - T_\infty| + C \cdot U_\infty + C \cdot U_\infty^2) \quad (1)$$



Fig. 1 – (a) Experimental small-scale greenhouse and (b) Building energy model (BEM)

Furthermore, the natural ventilation model used for the two roof operable vents is described by the quadrature sum of the wind-driven ventilation (Eq. 2) and the stack-driven ventilation (Eq. 3), where Q_w is the wind-driven volumetric air flow rate ($\text{m}^3\cdot\text{s}^{-1}$), C_w the opening effectiveness, A_{op} the opening area (m^2), U_∞ the local wind speed ($\text{m}\cdot\text{s}^{-1}$), Q_s the stack driven airflow rate ($\text{m}^3\cdot\text{s}^{-1}$), C_D the discharge coefficient, g the gravitational acceleration ($\text{m}^2\cdot\text{s}^{-1}$), ΔH_{NPL} is the height from midpoint of lower opening to the neutral pressure level (m).

$$Q_w = C_w A_{op} U_\infty \quad (2)$$

$$Q_s = C_D A_{op} \sqrt{2g\Delta H_{NPL}(|T_z - T_\infty|/T_z)} \quad (3)$$

3.2 Evidence-Based Calibration

The attributes of the greenhouse EnergyPlus model were specified using the principles of evidence-based energy model calibration, which is based on data collection and analysis (Raftery et al., 2011). Based on measurements, the lighting system power level was lowered from 3 400 W to 3 200 W. The heating setpoint was set at 15 °C for the thermal zone and 18 °C for the mean air temperature control of the hydronic heating radiant slab-on-grade system.

Data was gathered for 2022 using an independent acquisition system (Yokogawa GM10) that measures temperature, humidity inside the greenhouse, and hot water flow rate. Three current transducers are connected to a second acquisition system (EGauge EG4130) to monitor the electric energy consumption of the boiler, the fancoil, and the artificial lighting.

Unfortunately, the local weather station data was corrupted for a significant portion of 2022. The ERA5 reanalysis weather (Hersbach et al., 2020) and Copernicus Atmosphere Monitoring Service (CAMS) radiation service (Schroedter-Homscheidt et al., 2016) were used to generate the actual weather year (AWY) weather files. The boiler capacity was first adjusted based on measurements. The electric boiler is located in a technical shed next to the small-scale experimental greenhouse. A fraction of the boiler heating capacity dissipates inside the tech-

nical shed. The electrical boiler's thermal efficiency was adjusted to account for this. This was completed by comparing the thermal energy provided by the hydronic circuit to the greenhouse with the electrical energy consumption of the boiler. Regression analysis of the thermal energy against the electrical energy yielded a thermal efficiency of 88.35 % (R^2 of 0.98), as illustrated in Fig. 2. This ensured that the appropriate amount of thermal energy was supplied to the zone and that the total boiler electrical energy was adequately modelled.

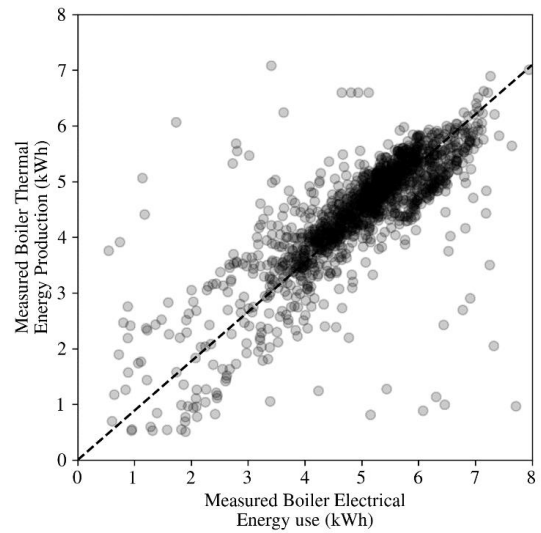


Fig. 2 – Measured boiler thermal energy as a function of measured boiler electrical energy

A blower door test yielded a $310 \text{ L}\cdot\text{s}^{-1}$ infiltration airflow rate at 50 Pascals. According to Eq. 4, the initial infiltration was thus set at 0.7 air changes per hour (ACH).

$$\text{ACH}_{\text{Natural}} \approx \frac{\text{ACH}_{50}}{20} \approx 0.7 \quad (4)$$

The calibration of the model was assessed using specific metrics, such as those proposed by ASHRAE Guideline 14-2014 (American Society of Heating and Engineers, 2014). This guideline states that a building energy model is deemed calibrated if the net mean bias error (NMBE) is below 5 % and the coefficient of variation of the root-mean-square error (CV-RMSE-) is below 15 % using monthly data, as defined by Eq. 5 and 6, respectively.

$$\text{NMBE} = \frac{\sum_{i=1}^n (y_i - \hat{y}_i)}{(n - p) \times \bar{y}} \times 100 \quad (5)$$

$$CV\text{-}RMSE = \left[\frac{\sum_{i=1}^n (y_i - \hat{y}_i)^2}{(n - p)} \right]^{1/2} / \bar{y} \times 100 \quad (6)$$

3.3 Model Parameter Estimation

Following the evidence-based calibration, additional parameters were estimated using an optimisation algorithm sometimes classified as an automated off-line calibration technique. The bottom slab thickness, the polystyrene insulation thickness, the concrete thermal conductivity and the infiltration model parameters were estimated using ExCal-iBem (Sansregret et al., 2014), an interface to the Genopt optimisation program (Wetter, 2001). The optimisation algorithm used is the hybrid particle swarm optimisation and Hooke-Jeeves generalised pattern search (GPSPSOCCHJ).

The optimisation problem used to estimate these parameters is stated in Eq. 7 with the two quadratic loss functions (Eq. 8 and 9). The objective function (Eq. 7) was computed over the monthly FCU energy, the monthly boiler energy and the total monthly energy in addition to the hourly FCU energy, boiler energy and temperature profiles for three periods of 2022: (1) February 12th to February 28th, (2) September 21st to October 5th and (3) December 12th to December 28th. These periods were selected to cover operating conditions where different systems were active: period (1) includes the FCU and hydronic floor, period (2) comprises the hydronic floor and

operable vents, and period (3) involves only the hydronic floor.

$$f(\mathbf{x}) = \frac{|NMBE| + CVRMSE}{C} \quad (7)$$

$$g_1(\mathbf{x}) = \max(0, |NMBE| - 5)^2 \quad (8)$$

$$g_2(\mathbf{x}) = \max(0, CVRMSE - 15)^2 \quad (9)$$

The parameters of the parameter vector (\mathbf{x}) are listed in Table 1, including their initial value, lower bound, upper bound, and step size. The initial values for the infiltration model (Eq. 1) were set using the values suggested by BLAST (Herron et al., 1981). The concrete thermal properties were taken from the ASHRAE fundamentals handbook (American Society of Heating and Engineers, 2021) ($\rho=2240 \text{ kg}\cdot\text{m}^{-3}$, $c_p=900 \text{ J}\cdot\text{kg}^{-1}\cdot\text{K}^{-1}$). The concrete slab is 0.75 m deep at its thickest point and is at least 3 inches (0.076 m) deep under the radiant hydronic slab.

4. Results

Table 1 presents the parameter estimates obtained using the optimisation algorithm. Fig. 3 presents the measured and simulated monthly energy consumption of the FCU, boiler, and lighting system. The energy model is deemed calibrated at a monthly level according to ASHRAE Guideline-14 with a NMBE of 1.90 % and a CV-RMSE of 5.75 %.

Table 1 – Estimated parameter initial value, lower bound, upper bound, step size and estimated value.

Parameter	Initial value	Lower bound	Upper bound	Step Size	Estimated Value
$k_{slab} \text{ (W}\cdot\text{m}^{-1}\cdot\text{K}^{-1})$	2.0	1.3	2.6	0.1	1.56
$L_{slab} \text{ (m)}$	0.750	0.076	0.750	0.001	0.5822
$k_{ins} \text{ (W}\cdot\text{m}^{-1}\cdot\text{K}^{-1})$	0.029	0.029	25	0.001	15.43
A	0.606	0	10	0.01	6.66
$B \text{ (K}^{-1})$	0.03606	0	0.50	0.0001	0.06263
$C \text{ (s}\cdot\text{m}^{-1})$	0.117	0	0.50	0.0001	0.4292
$D \text{ (s}^2\cdot\text{m}^2)$	0.000	0	0.005	0.0001	0.0018344
$\Delta H_{NPL} \text{ (m)}$	4.2	0	10	0.01	6.95
C_w	0.5	0	1	0.01	0.9938
C_D	0.5	0	1	0.01	0.54938

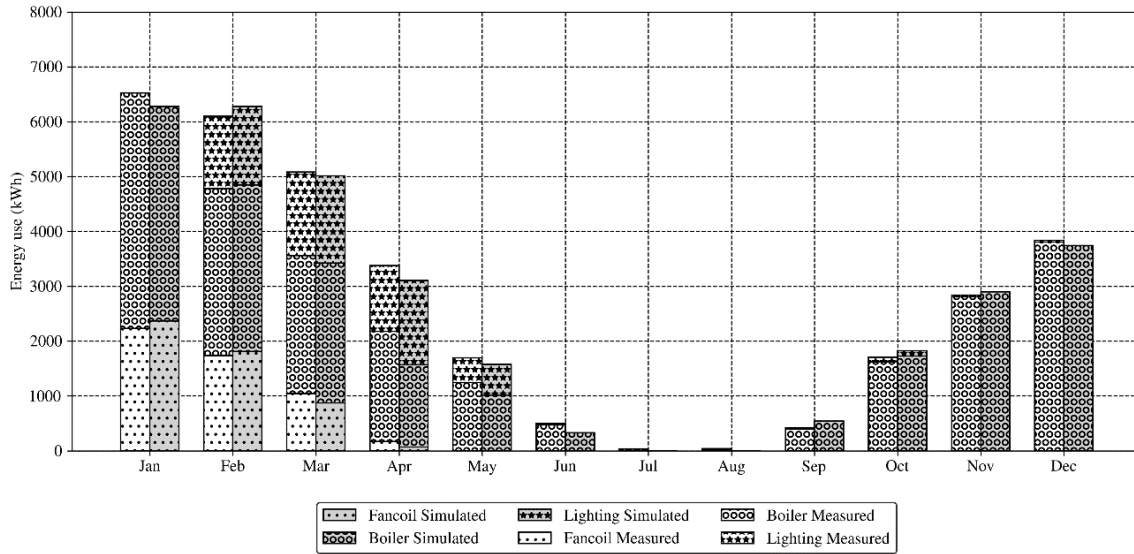


Fig. 3 – Monthly measured and simulated energy use for the year 2022

Fig. 4 and Fig. 5 show the measured and simulated hourly temperatures and relative humidity, respectively. Upon analysis of the data, it appeared that the temperature measured inside the greenhouse seemed unusually high for certain measured data points (Fig. 4). The likely explanation for this was that the installed thermocouples were left unshielded for the 2022 calendar year, leading to elevated readings during sunny periods.

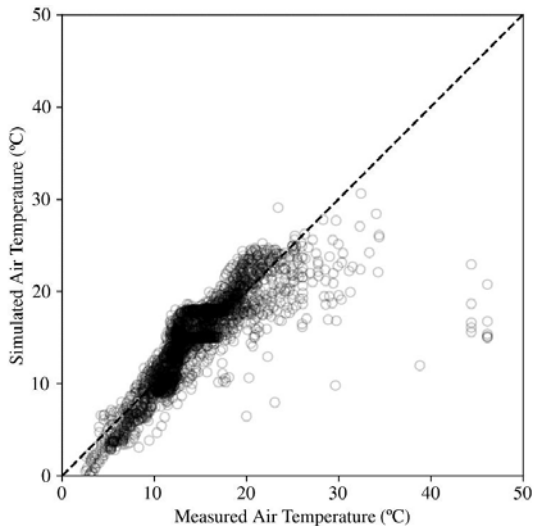


Fig. 4 – Simulated and measured air temperature inside the greenhouse in 2022

evident that the heating systems' capacity was insufficient during part of 2022, as the measured temperature dropped below the lower safety setpoint of 15 °C. Since the heating system's capacity was modelled according to the design data, the model also demonstrated temperatures that fell below the safety setpoint programmed into the heating systems, as depicted in Fig. 4. Additional heating capacity is being installed to resolve this issue.

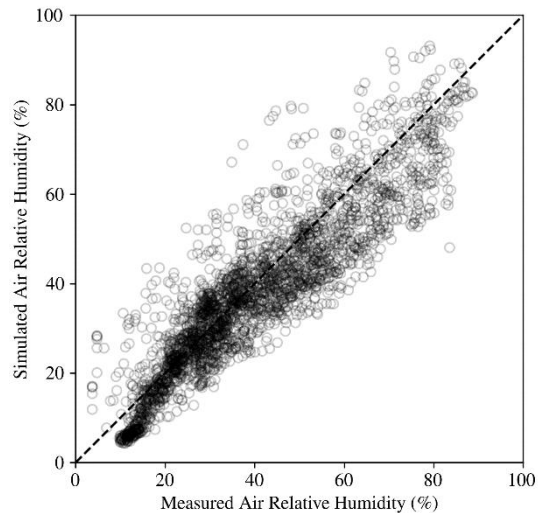


Fig. 5 – Simulated and measured relative humidity inside the greenhouse in 2022

Also, upon inspecting the left portion of Fig. 4, it is

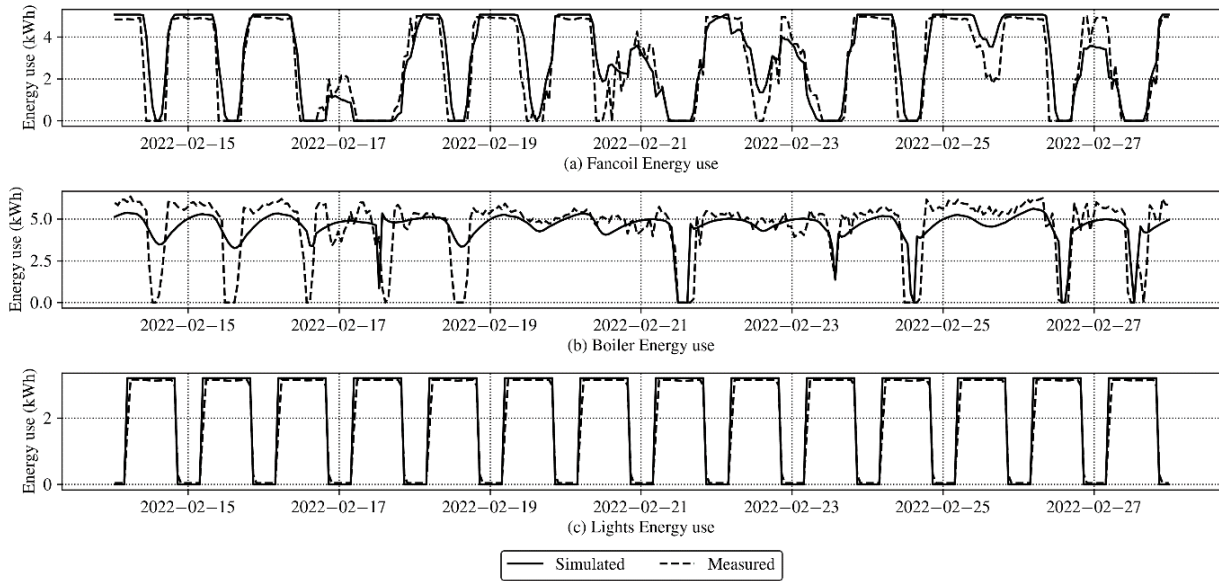


Fig. 6 – Hourly measured and simulated FCU, boiler and lighting energy use from February 14th 2022 to February 27th 2022

Prediction performance metrics were not computed on temperature and humidity measurements, as they are shown to be flawed. Hence, Fig. 4 and Fig. 5 are provided as a general indication of the agreement between simulated and measured temperature and relative humidity data. Further work will be undertaken to provide the scientific community with accurately calibrated energy models.

Fig. 6 presents the hourly energy consumption profiles of the energy systems for a typical week where the FCU, the hydronic floor system and the lighting systems are in operation. The energy consumption of the lighting system follows a regular pattern and can easily be modelled using a power level and a schedule. Improvements are still needed in modelling the hydronic floor and the FCU. These two systems did not use the same sensor for control, which is believed to contribute to the discrepancies between the measured and simulated data. The control system will be adjusted to link the operation of both systems based on the same sensor reading.

5. Discussion

The presented results highlight the importance of being cautious when selecting the parameters, as the optimisation problem could become ill-posed, resulting in considerably different parameter esti-

mates with even small changes in the objective function. Conducting a sensitivity analysis to identify the influential parameters, rather than relying on the heuristic method, would be valuable in developing a more robust calibration approach. The parameters of the infiltration model estimated using the meta-heuristic optimisation algorithm could be verified through tracer gas decay experiments using the procedure described in ASTM E741-11. Conducting these experiments under various weather conditions would yield the necessary data to derive empirical correlation coefficients for the greenhouse-specific infiltration model. This could be repeated in greenhouses with different shapes, dimensions, and constructions to support the development of reference values for future modellers.

The estimated opening effectiveness (C_w) values obtained through the optimisation algorithm should be validated in future studies, as such high opening effectiveness is unusual. This could be attributed to the combination of a small-scale greenhouse with relatively large roof vent openings.

Improvement to the weather data used could also be achieved by using a dedicated site weather station. This additional data source will include many on-site measurements such as outdoor temperature, relative humidity (Campbell Scientific HMP45C), carbon dioxide (Vaisala GMP343), wind speed and

direction (05103VK-L), global shortwave irradiance (EKO MS-80SH pyranometer), barometric pressure (Campbell Scientific CS100) and rain and snow (R.M. Young 52202). Furthermore, microclimate measurements within the greenhouse will be added, such as temperature (Apogee TS-100), radiation-shielded thermocouples, relative humidity, carbon dioxide, net radiometers (apogee SN-522-SS), PAR (apogee SQ-500-SS) and ePAR (apogee SQ-610-SS) are installed.

Once the data with crops inside the greenhouse becomes available, the calibration of the greenhouse energy model should be revised, integrating a canopy-level heat balance algorithm. This integration will consider the sensible and latent heat exchanges between the crops and the greenhouse microclimate.

6. Conclusion

This paper presents the calibration results of a building energy model for controlled environment agriculture (CEA) using real-world measurements from a highly instrumented small-scale experimental greenhouse. Further analysis of the simulated and measured temperature profiles should offer additional insights into the model calibration approach. The next step will involve gathering data on crop hygrothermal loads within the greenhouse, integrating the crop leaf-level energy balance into the simulation engine and continuing the calibration process.

Nomenclature

Symbols

A_{op}	opening area (m ²)
C_D	discharge coefficient
C_w	opening effectiveness
\hat{y}	estimated data
ΔH_{NPL}	midpoint height from the lower opening to the neutral pressure level (m)
I	infiltration flow rate (ACH)
Q	volumetric flow rate (m ³ ·s ⁻¹)
T	temperature (°C)

U	wind speed (m·s ⁻¹)
g	gravitational acceleration (m ² ·s ⁻¹)
n	number of data points
p	number of parameters
y	measured data

Subscripts/Superscripts

∞	outside
D	design
s	stack-driven
w	wind-driven
z	zone

References

- American Society of Heating, Refrigerating, and Air-Conditioning Engineers. 2014. "Guideline 14-2014: measurement of energy, demand, and water savings."
- American Society of Heating, Refrigerating, and Air-Conditioning Engineers. 2021. *ASHRAE Handbook - Fundamentals*: American Society of Heating Refrigerating and Air-Conditioning Engineers Inc. <https://www.ashrae.org/technical-resources/ashrae-handbook/description-2021-ashrae-handbook-fundamentals>
- Beaulac, Arnaud, Danielle Monfet, and Didier Haillot. 2023. "Revue de la modélisation énergétique de serres avec TRNSYS." Conférence SFT.
- Crawley, Drury B, Linda K Lawrie, Frederick C Winkelmann, Walter F Buhl, Y Joe Huang, Curtis O Pedersen, Richard K Strand, Richard J Liesen, Daniel E Fisher, and Michael J Witte. 2001. "EnergyPlus: creating a new-generation building energy simulation program." *Energy and buildings* 33 (4): 319-331.
- Guglielmetti, Rob, Dan Macumber, and Nicholas Long. 2011. "OpenStudio: an open source integrated analysis platform." <https://www.nrel.gov/docs/fy12osti/51836.pdf>
- Graamans L, Baeza E, van den Dobbelen A, Tsafaras I, Stanghellini C. 2018. "Plant factories versus greenhouses: Comparison of resource use efficiency." *Agricultural Systems* (160):31-43.

- Herron, Dale, George Walton, and Linda Lawrie. 1981. *Building loads analysis and system thermodynamics (BLAST) program users manual. Volume one. Supplement (Version 3.0)*. Illinois, IL: US Army Construction Engineering Research Laboratory (CERL).
- Hersbach, Hans, Bill Bell, Paul Berrisford, Shoji Hirahara, András Horányi, Joaquín Muñoz-Sansregret, Simon, Karine Lavigne, Ahmed Daoud, and Louis-Alexandre Leclaire. 2014. "ExCalibBEM Tool Development to Calibrate Building Energy Models." Proceedings of eSim 2014: 8th Conference of IBPSA-Canada.
- Schroedter-Homscheidt, Marion, Antti Arola, Niels Killius, Mireille Lefèvre, Laurent Saboret, Sabater, Julien Nicolas, Carole Peubey, Raluca Radu, and Dinand Schepers. 2020. "The ERA5 global reanalysis." *Quarterly Journal of the Royal Meteorological Society* 146 (730): 1999-2049.
- Raftery, Paul, Marcus Keane, and James O'Donnell. 2011. "Calibrating whole building energy models: An evidence-based methodology." *Energy and Buildings* 43 (9): 2356-2364..
- William Wandji, Lucien Wald, and Etienne Wey. 2016. "The Copernicus atmosphere monitoring service (CAMS) radiation service in a nutshell." 22nd SolarPACES Conference 2016.
- Wetter, Michael. 2001. "GenOpt –A Generic Optimization Program." Proceedings of BS 2001: 7th international IBPSA conference.